

Anomalous pinning in superconductors with strong Pauli paramagnetism

Y. Ōnuki, M. Hedo, Y. Inada, R. Settai, H. Sugawara, Y. Aoki, H. Sato, M. Deppe, Philipp Gegenwart, C. Geibeld, M. Lang, T. Lühmann, R. Modler, M. Weiden, F. Steglich, C. Paulsen, J. L. Tholence, N. Sato, T. Komatsubara, M. Tachiki, S. Takahashi

Angaben zur Veröffentlichung / Publication details:

Ōnuki, Y., M. Hedo, Y. Inada, R. Settai, H. Sugawara, Y. Aoki, H. Sato, et al. 1996.
"Anomalous pinning in superconductors with strong Pauli paramagnetism." *Physica B: Condensed Matter* 223-224: 28–32. [https://doi.org/10.1016/0921-4526\(96\)00030-0](https://doi.org/10.1016/0921-4526(96)00030-0).

Anomalous pinning in superconductors with strong Pauli paramagnetism

Y. Ōnuki^{a, b, *}, M. Hedo^a, Y. Inada^a, R. Settai^a, H. Sugawara^c, Y. Aoki^c, H. Sato^c, M. Deppe^d, P. Gegenwart^d, C. Geibel^d, M. Lang^d, T. Lühmann^d, R. Modler^d, M. Weiden^d, F. Steglich^d, C. Paulsen^e, J.L. Tholence^e, N. Sato^f, T. Komatsubara^f, M. Tachiki^g, S. Takahashi^g

^a Faculty of Science, Osaka University, Toyonaka, Osaka 560, Japan

^b Advanced Science Research Center, Japan Atomic Energy Research Institute, Tokai, Ibaraki, 319-11, Japan

^c Faculty of Science, Tokyo Metropolitan University, Minami-Osawa 1-1, Hachioji, Tokyo 192-03, Japan

^d Institut für Festkörperphysik, SFB 252, TH Darmstadt, D-64289 Darmstadt, Germany

^e CRTB, CNRS, F-38042 Grenoble Cedex 9, France

^f Department of Physics, Faculty of Science, Tohoku University, Sendai 980, Japan

^g Institute for Materials Research, Tohoku University, Sendai 980, Japan

Abstract

The results of the magnetization, magnetostriction and AC-susceptibility experiments are presented for both the antiferromagnetic heavy-Fermion superconductor UPd₂Al₃ and the valence fluctuation compound CeRu₂. For ($H > 10$ kOe). These results are discussed on the basis of a generalized Fulde–Ferrell–Larkin–Ovchinnikov superconducting state.

Heavy-Fermion compounds in the f-electron systems have attracted much attention because of their superconducting properties. For example, UPt₃ is well-known to exhibit two critical temperatures and three phases called A, B and C in the superconducting H – T phase diagram [1]. The existence of multiple superconducting phases is reminiscent of superfluid ³He and is very strong evidence that UPt₃ is a superconductor with reduced symmetry.

UPd₂Al₃ is a hexagonal compound, which also shows fascinating superconducting properties. It exhibits co-existence of heavy-Fermion superconductivity ($T_c \leq 2$ K) and strong antiferromagnetic order ($T_N = 14.5$ K) [2]. Modler et al. reported a few years ago anomalies in the sample length $l(T, H)$ within the superconducting state, pointing to a first-order phase transition at H_1^*

($10 \text{ kOe} < H_1^* < H_{c2}(0) = 35 \text{ kOe}$) and $T < 0.8 T_c$ [3]. Gloos et al. subsequently discussed these anomalies in terms of a first-order phase transition from the mixed state to an inhomogeneous superconducting state [4] as theoretically proposed by Fulde and Ferrell (FF) [5] and independently by Larkin and Ovchinnikov (LO) [6].

More than three decades ago these authors proposed that in a very clean and strongly Pauli-limited singlet superconductor, a partially polarized superconducting state should form at high magnetic fields. This spatially modulated FFLO state should raise the upper critical field H_{c2} at which the superconducting-normal transition takes place. While the FFLO state was unsuccessfully searched for among classical superconductors, there have been recent claims for its existence in certain heavy-Fermion superconductors. UPd₂Al₃ fully meets the following strict requirements: It is (1) a clean superconductor

* Corresponding author.

(the electronic mean free path $l = 700 \text{ \AA} \gg$ the coherence length $\xi = 85 \text{ \AA}$) and (2) subject to strong Pauli limiting ($H_{c2}(0) = H_p$ [in 10 kOe] = 1.84 T_c [in K]).

Besides UPd_2Al_3 , CeRu_2 with the cubic Laves phase structure is known to show similar behavior [7–10]. The critical temperature is rather high, $T_c = 6.2 \text{ K}$. CeRu_2 is a valence-fluctuation compound where the f electron is itinerant, contributing the conduction electrons at low temperatures. The electronic specific heat coefficient γ is enhanced, 30 mJ/mol K^2 . Therefore, the upper critical field H_{c2} is large 60–70 kOe, and then the coherence length is short, 60–70 \AA .

In this paper we present the results of magnetization, magnetostriction and AC-susceptibility measurements for UPd_2Al_3 and CeRu_2 as well as AC-susceptibility measurements for CeCo_2 . As for CeRu_2 , we have determined the electronic mean free path via de Haas–van Alphen effect measurements to give evidence that CeRu_2 is a clean superconductor, too. Below, we discuss unique anomalies associated with a first-order phase transition.

Fig. 1 shows the magnetization at 0.15 K in UPd_2Al_3 . At low fields, a very sharp peak in the magnetization is found at the lower critical field H_{c1} , which is of the order of 100 Oe only. Furthermore, a hysteretic peak in the magnetization curve shows up above H_i^* as high as about 30 kOe, as shown in an inset of Fig. 1. Here the data denoted by the open/closed circles are taken upon moving the sample up/down within the pick-up coils of the magnetometer. The anomaly resembles the shape of magnetization loops found in superconductors with a pronounced peak effect. Most remarkably, the magnetization process is reversible over a wide field range, i.e. $10 \text{ kOe} < H < H_i^*$. Such a reversible magnetization curve is highly unusual and has only been observed in extremely clean type-II superconductors, e.g., in $\text{Nb}(\kappa = 0.8)$ with a residual resistivity ratio of 1830 [11]. This indicates that the pinning force for the magnetic vortices is very weak. On the other hand, the occurrence of the peak effect above H_i^* even for large value of $\kappa = 50$, highlights a very strong pinning force in UPd_2Al_3 . The transition between the weak pinning region and the strong one is of a first order, as discussed previously from the results of high-precision length measurements [4].

Fig. 2 shows the corresponding magnetization curve for CeRu_2 . The data denoted by open circles were obtained by increasing the field after zero-field cooling, while those by triangles were obtained by decreasing the field. The magnetization in the mixed state is also reversible in a wide field range from 10 kOe to H_i^* ($= 38 \text{ kOe}$) at 2.25 K. On the other hand, there is found an irreversible peak structure in the field range from H_i^* to H_i^* ($= 52 \text{ kOe}$).

When the temperature approaches the critical temperature, i.e. for $T > 0.8 T_c$, no such peak structure is

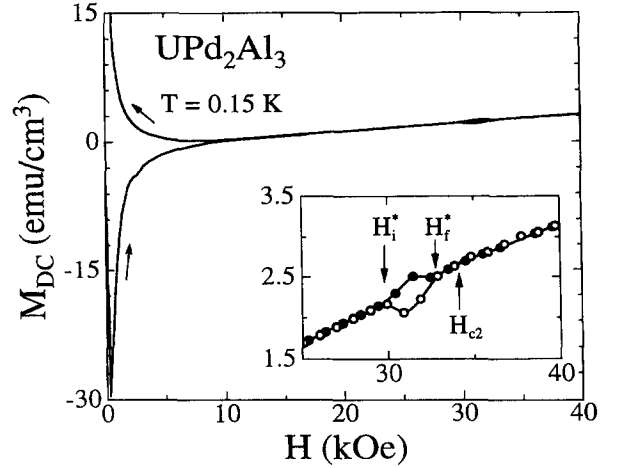


Fig. 1. Isothermal magnetization curve for UPd_2Al_3 . The inset shows the magnetization near H_{c2} .

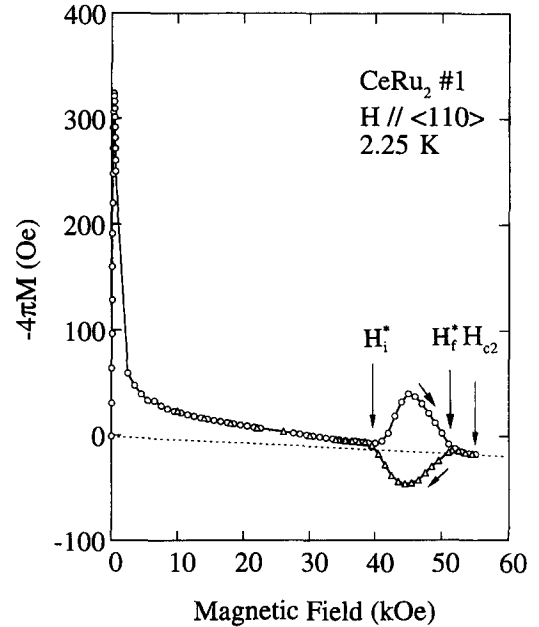


Fig. 2. Isothermal magnetization curve for CeRu_2 .

observed in the magnetization, as shown in Fig. 3. In this temperature region, the magnetization is reversible in the mixed state.

Fig. 4 shows the magnetostriction $\Delta l(H)$ of CeRu_2 at various temperatures. The observation of an abrupt change from a smooth and almost reversible magnetization process for $H < H_i^*$ to a behavior with pronounced field-induced length changes of hysteretic nature above

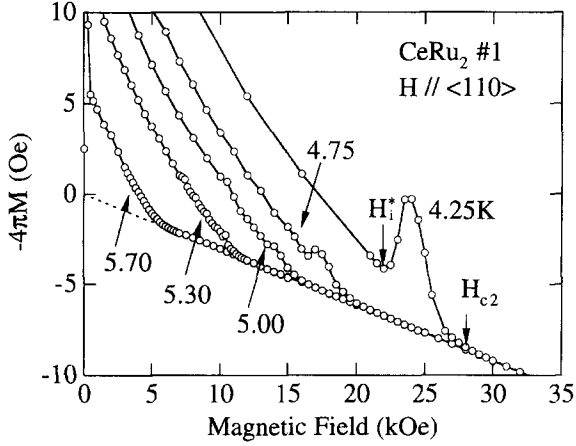


Fig. 3. Isothermal magnetization curves at differing temperatures for CeRu₂.

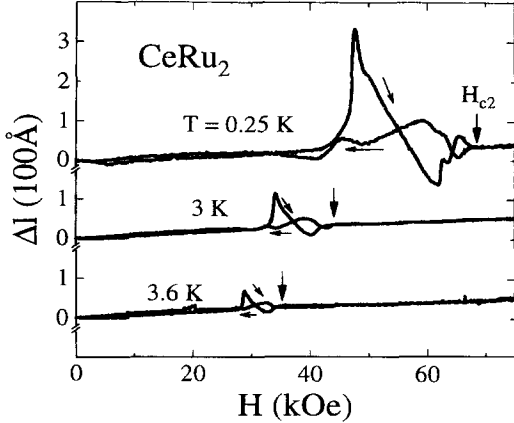


Fig. 4. Isothermal magnetostriction curves at differing temperatures for CeRu₂.

H_1^* strongly hints at the onset of flux pinning, i.e., at a pronounced coupling of the vortex lattice to the crystal lattice above H_1^* .

The strong decrease in amplitude of the $\Delta l(H)$ anomaly with increasing temperature has also been observed for UPd₂Al₃. As can be seen in Fig. 4 the anomalous structure in $\Delta l(H)$ becomes very small at 3.6 K, and for temperatures above 5.5 K, corresponding to $T/T_c = 0.9$, no anomaly can be resolved anymore, consistent with the magnetization results mentioned above. The abrupt increase of flux pinning above H_1^* , and moreover, the significant hysteresis in H_1^* upon increasing and decreasing field are strong indications for a first-order transition at H_1^* .

Reversible magnetization curves in UPd₂Al₃ and CeRu₂ below H_1^* indicate that the pinning force for the magnetic vortices is very weak. First we discuss the origin of the small pinning force. UPd₂Al₃ and CeRu₂ exhibit large spin susceptibilities, $\chi_p = 3.2 \times 10^{-5}$ and 2.2×10^{-5} emu/cm³, respectively. Therefore, the quasi-particles inside the vortex cores gain a large Zeeman energy which, close to H_{c2} , becomes comparable to the superconducting condensation energy $H_c^2/8\pi = 0.25(\gamma/V_{\text{mol}})T_c^2$, where H_c is the thermodynamic critical field, the electronic specific heat coefficient γ (125 and 30 mJ/mol K², respectively) and V_{mol} the molar volume (62.94 and 32.23 cm³/mol, respectively). Consequently, one estimates a very small self-energy of the vortex, $E_{\text{core}} = \pi\xi^2[H_c^2/8\pi - (1/2)\chi_p h^2]$, h being the magnetic field induced at the vortex core by the shielding currents surrounding it. This explains the weak pinning of vortices in a wide field range below H_1^* .

We show in Fig. 5 the phase diagrams for both UPd₂Al₃ and CeRu₂. Here H_1^* and H_2^* indicate the onset and offset fields of irreversibilities, see Figs. 1 and 2. These phase diagrams are obtained from the magnetization, length and AC-susceptibility measurements.

A similar phase diagram has been recently obtained from the AC-susceptibility experiments for CeCo₂, as shown in Figs. 6 and 7. This compound is also a valence fluctuation compound similar to CeRu₂, where $T_c = 1.4$ K, $\gamma = 35$ mJ/K² mol, $\xi = 350$ Å and $l > 1000$ Å. The itinerant 4f electron exhibits a relatively large mass of $11m_0$ [12].

For the dotted region of the phase diagram in UPd₂Al₃, the FFLO state was discussed previously [4]. Tachiki et al. have recently proposed a generalized FFLO state, where the parameter is spatially modulated, and planar nodes of the order parameter are periodically aligned perpendicular to the vortices [13]. A schematic diagram of the generalized FFLO state is shown in Fig. 8, in which the solid lines show the center of the vortices and the dashed lines show the planar nodes of the superconducting order parameter perpendicular to the vortices. The occurrence of planar nodes of the order parameter leads to a segmentation of the vortices into pieces with a length Λ which is one order of magnitude larger than the coherence length. As a result, these vortex segments become flexible in a qualitatively similar way as the quasi-two-dimensional vortex disks (pancakes) in cuprate superconductors [14]. The flexible vortices are collectively pinned by the weak pinning centers, producing the peak structure mentioned above.

The generalized FFLO state exists in a clean superconductor with large spin susceptibility and large κ . We have determined the electronic mean free path in CeRu₂ via de Haas-van Alphen oscillations. Fig. 9 shows the typical dHvA oscillation both in the superconducting mixed

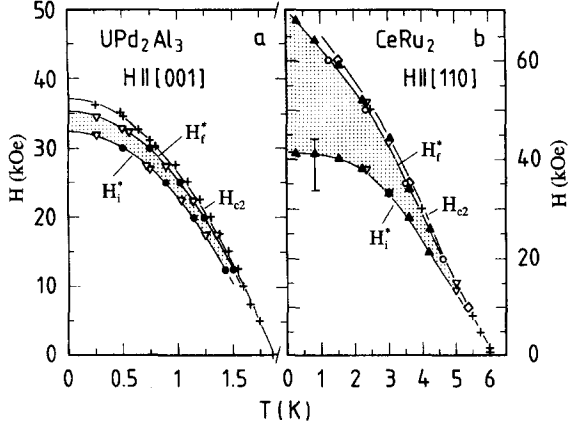


Fig. 5. H - T phase diagrams for superconducting UPd_2Al_3 and CeRu_2 .

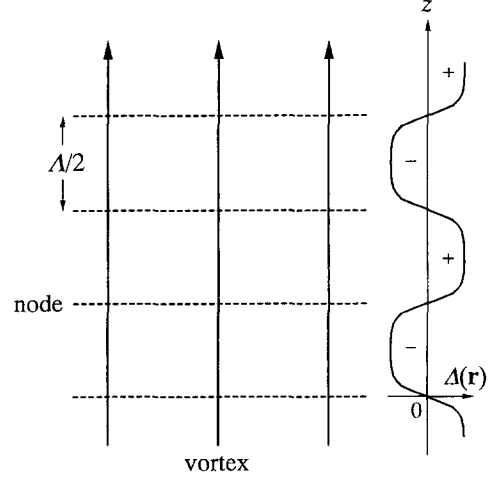


Fig. 8. Schematic diagram of the generalized FFLO state.

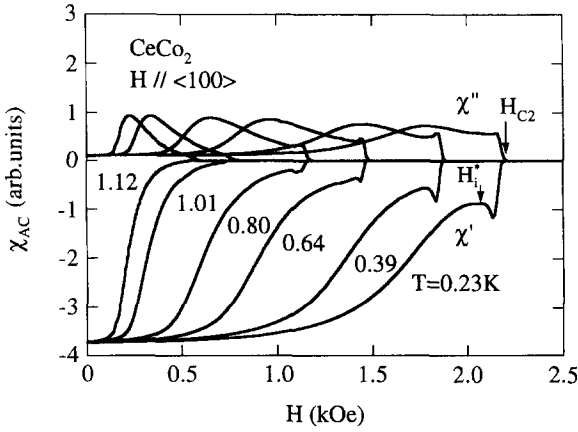


Fig. 6. Isothermal AC-susceptibility curves at differing temperatures for CeCo_2 .

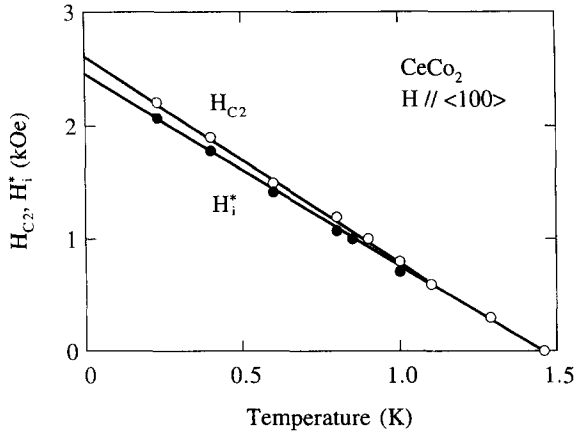


Fig. 7. H - T phase diagram for superconducting CeCo_2 .

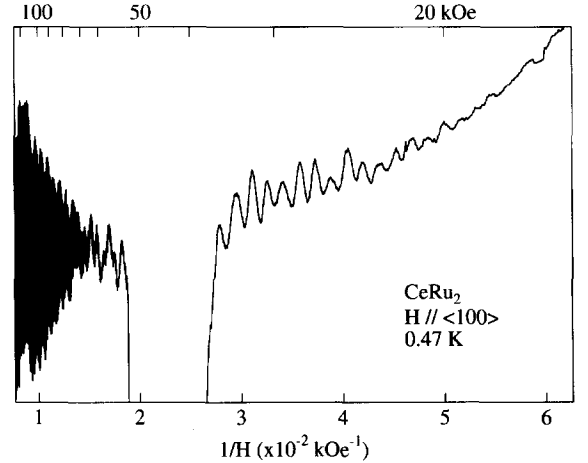


Fig. 9. dHvA oscillations both in the normal and mixed superconducting states for CeRu_2 .

state and the normal state for the field along the $[100]$ direction at 0.47 K. A region between 40 and 55 kOe corresponds to the generalized FFLO state mentioned above, showing sharp drops in the oscillatory curve. Two or three branches are observed. The main dHvA frequency F is 2.28×10^7 Oe. We have determined the mean free path l for the carrier, using the following formulae; $S = \pi k_F^2$, $\hbar k_F = m_c^* v_F$ and $l = v_F \tau$. Here S is the cross-sectional area of the Fermi surface which is proportional to the dHvA frequency F ($= \hbar S / 2\pi e$), k_F the Fermi wave number, v_F the Fermi velocity, m_c^* the cyclotron effective mass and τ the scattering lifetime. From the temperature and field dependences of the dHvA amplitude, we can determine the cyclotron effective mass ($2.56 m_0$) and the

scattering lifetime (1.13×10^{-12} s), respectively. From these values, we can estimate the mean free path $l = 1340$ Å. CeRu₂ is thus a very clean superconductor. We should like to note that the detected dHvA branches are well-explained by the 4f-itinerant band model [15].

We have presented magnetization, magnetostriction and AC-susceptibility results for UPd₂Al₃ and CeRu₂ as well as AC-susceptibility results for CeCo₂, indicating a first-order phase transition between weak and strong pinning. The origin of the strong pinning mechanism was discussed on the basis of the generalized FFLO superconducting state. We expect that there are more candidates for the generalized FFLO superconductor because usually, heavy-Fermion compounds show large spin susceptibilities and large κ values. We advocate that UBe₁₃ [16] and UPt₃ [17] might be promising materials, while UNi₂Al₃ is not [18]. Further experimental studies are necessary, especially to observe directly the unique nodal structure of the generalized FFLO order parameter.

We are grateful to T. Fujita, T. Suzuki, P. Fulde and D. Rainer for stimulating conversations. This work was supported by Grant-in-Aid for the Scientific Research from Ministry of Education, Science and Culture, Japan and by the SFB 252 Darmstadt/Frankfurt/Mainz. R.M. gratefully acknowledges a fellowship by the Forschungszentrum Karlsruhe-Technik und Umwelt.

References

- [1] S. Adenwalla, S.W. Lin, Z. Zhao, Q.Z. Ran, J.B. Ketterson, J.A. Sauls, L. Taillefer, D.G. Hinks, M. Levy and B.K. Sarma, Phys. Rev. Lett. 65 (1990) 2298.
- [2] C. Geibel, C. Schank, S. Thies, H. Kitazawa, C.D. Bredl, A. Böhm, M. Rau, A. Grauel, R. Caspary, R. Helfrich, U. Ahlheim, G. Weber and F. Steglich, Z. Phys. B 84 (1991) 1.
- [3] R. Modler, K. Gloos, C. Geibel, T. Komatsubara, N. Sato, C. Schank and F. Steglich, Int. J. Mod. Phys. B 7 (1993) 42.
- [4] K. Gloos, R. Modler, H. Schimanski, C.D. Bredl, C. Geibel, F. Steglich, A.I. Buzdin, N. Sato and T. Komatsubara, Phys. Rev. Lett. 70 (1993) 501.
- [5] P. Fulde and R.A. Ferrell, Phys. Rev. 135 (1964) 550.
- [6] A.I. Larkin and Yu.N. Ovchinnikov, Soc. Phys. JETP 20 (1965) 762.
- [7] K. Yagasaki, M. Hedo and T. Nakama, J. Phys. Soc. Japan 62 (1993) 3825.
- [8] A.D. Huxley, C. Paulsen, O. Laborde, J.L. Tholence, D. Sanchez, A. Junod and R. Calemczuk, J. Phys.: Condens. Matter 5 (1993) 7709.
- [9] H. Sugawara, T. Yamazaki, N. Kimura, R. Settai and Y. Ōnuki, Physica B 206–207 (1995) 196.
- [10] H. Goshima, T. Suzuki, T. Fujita, M. Hedo, T. Nakma and K. Yagasaki, Physica B 206–207 (1995) 193.
- [11] D.K. Finnemore, T.F. Stromberg and C.A. Swenson, Phys. Rev. 149 (1966) 231; C. Lau, M. Schachinger, M. Prohammer, A. Junod and D. Eckert, Phys. Rev. B 44 (1991) 7858.
- [12] H. Sugawara, O. Inoue, Y. Kobayashi, H. Sato, T. Nishigaki, Y. Aoki, H. Sato, R. Settai and Y. Ōnuki, J. Phys. Soc. Japan 64 (1995) 3639.
- [13] M. Tachiki, S. Takahashi, P. Gegenwart, M. Weiden, M. Lang, C. Geibel, F. Steglich, R. Modler, C. Paulsen and Y. Ōnuki, Z. Phys. B., in press.
- [14] W.K. Kwok, J.A. Fendrich, C.J. van der Bek and G.W. Crabtree, Phys. Rev. Lett. 73 (1994) 2614.
- [15] M. Hedo, Y. Inada, T. Ishida, E. Yamamoto, Y. Haga, Y. Ōnuki, M. Higuchi and H. Hasegawa, J. Phys. Soc. Japan 64 (1995) 4535.
- [16] F. Thomas et al., J. Low. Temp. Phys., in press.
- [17] K. Tenya, M. Ikeda, T. Tayama, H. Mitamura, H. Amit-suka, T. Sakakibara, K. Maezawa, N. Kimura, R. Settai and Y. Ōnuki, J. Phys. Soc. Japan 64 (1995) 1063.
- [18] R. Modler, Dissertation, Darmstadt (1995), unpublished.